

Syntheses and Characterizations of a Series of Novel $\text{Ln}_6\text{Cu}_{24}$ Clusters with Amino Acids as LigandsJian-Jun Zhang,[†] Tian-Lu Sheng,[†] Sheng-Qin Xia,[†] Guido Leibelng,[‡] Franc Meyer,[‡] Sheng-Min Hu,[†] Rui-Biao Fu,[†] Sheng-Chang Xiang,[†] and Xin-Tao Wu^{*†}

State Key Laboratory of Structural Chemistry, Fujian Institute of Research on the Structure of Matter, Chinese Academy of Sciences, Fuzhou, Fujian 350002, P. R. China, and Institut fuer Anorganische Chemie der George-August-Universitaet Goettingen, Tammannstrasse 4, 37077 Goettingen, Germany

Received March 7, 2004

With glycine or L-alanine as ligands, a series of novel 3d–4f heterometallic $\text{Ln}_6\text{Cu}_{24}$ clusters with the formulas of $[\text{Sm}_6\text{Cu}_{24}(\mu_3\text{-OH})_{30}(\text{Gly})_{12}(\text{Ac})_{12}(\text{ClO}_4)(\text{H}_2\text{O})_{16}] \cdot (\text{ClO}_4)_9 \cdot (\text{OH}) \cdot (\text{H}_2\text{O})_{31}$ (**1**) and $[\text{Ln}_6\text{Cu}_{24}(\mu_3\text{-OH})_{30}(\text{Ala})_{12}(\text{Ac})(\text{ClO}_4)(\text{H}_2\text{O})_{12}] \cdot (\text{ClO}_4)_{10} \cdot (\text{OH})_7 \cdot (\text{H}_2\text{O})_{34}$ (**2**·Ln) (Ln = Tb, Gd, Sm, and La) were synthesized by self-assembly, among which **1** and **2**·Tb were characterized by X-ray structure analysis. The metal skeleton of the clusters may be described as a huge $\{\text{Ln}_6\text{Cu}_{12}\}$ octahedron (constructed with 6 Ln^{III} ions located at the vertices and 12 inner Cu^{II} ions located at the midpoints of the edges) connected by 12 additional Cu^{II} ions (every 2 are connected to 1 Ln^{III} vertex). The temperature dependence of the magnetic susceptibilities of **2**·Ln was investigated and was found to vary with the central rare-earth ions. Impedance spectroscopic measurements of **2**·Ln reveal that they are ionic conductors.

Introduction

Recently, high-nuclear metal clusters (metal clusters with many nuclei) have attracted much attention in several fields owing to their fascinating structures and interesting properties,¹ among which perhaps the most interesting and important cluster is $\{\text{Mo}_{368}\}$ reported by Müller.² Other famous examples of large clusters are $\{\text{Ag}_{188}\}$,^{3(a)} $\{\text{Cu}_{146}\}$,^{3(b)} $\{\text{Pd}_{145}\}$,⁴ and $\{\text{Mn}_{30}\}$.⁵ These high-nuclear clusters are known not only for their unusual physical and chemical properties inherited from small building blocks^{1b} but also for their nanoscopic dimension; for example, the quantum tunnel effect observed in the well-known $\{\text{Mn}_{12}\}$ cluster.⁶}}

* Author to whom correspondence should be addressed. Fax: 86-591-3714947. Tel: 86-591-3719238. E-mail: wxt@ms.fjirsm.ac.cn.

[†] Chinese Academy of Sciences.

[‡] Institut fuer Anorganische Chemie der George-August-Universitaet Goettingen.

- (1) (a) Winpenny, R. E. P. *Chem. Soc. Rev.* **1998**, 27, 447; (b) Müller, A.; Serain, C. *Acc. Chem. Res.* **2000**, 33, 2.
- (2) Müller, A.; Beckman, E.; Bögge, H.; Schmidtman, M.; Dress, A. *Angew. Chem., Int. Ed.* **2002**, 41, 1162.
- (3) (a) Wang, X.-J.; Langetepe, T.; Persau, C.; Kang, B.-S.; Sheldrick, G. M.; Fenske, D. *Angew. Chem., Int. Ed.* **2002**, 41, 3818; (b) Krautscheid, H.; Fenske, D.; Baun, G.; Semmelmann, M. *Angew. Chem., Int. Ed. Engl.* **1993**, 32, 1303.
- (4) Tran, N. T.; Powell, D. R.; Dahl, L. D. *Angew. Chem., Int. Ed.* **2000**, 39, 4121.
- (5) Soler, M.; Wernsdorfer, W.; Folting, K.; Pink, M.; Christou, G. *J. Am. Chem. Soc.* **2004**, 126, 2156.

Since 1985,⁷ the design and characterization of 3d–4f heterometallic complexes has been an interesting research area, and many complexes with a low-nuclear (clusters with few nuclei), chain, and net structural motif have been reported.⁸ But for 3d–4f heteronuclear clusters with seven or more metal ions, only six 7-nuclear LnM_6 (M means transition metal) clusters,⁹ one 10-nuclear Ln_2Cu_8 cluster,¹⁰ one 18-nuclear $\text{Ln}_6\text{Cu}_{12}$ cluster,¹¹ one 20-nuclear $\text{La}_8\text{Cu}_{12}$

- (6) Boyd, P. D. W.; Li, Q.; Vincent, J. B.; Folting, K.; Chang, H. R.; Streib, W. E.; Huffmann, J. C.; Christou, G.; Hendrickson, D. N. *J. Am. Chem. Soc.* **1988**, 110, 8537.
- (7) Bencini, A.; Benelli, C.; Caneschi, A.; Carlin, R. L.; Dei, A.; Gatteschi, D. *J. Am. Chem. Soc.* **1985**, 107, 8128.
- (8) (a) Benelli, C.; Gatteschi, D. *Chem. Rev.* **2002**, 102, 2369, and references therein. (b) Sakamoto, M.; Manseki, K.; Okawa, H. *Coord. Chem. Rev.* **2001**, 219–221, 379, and references therein.
- (9) (a) Yukawa, Y.; Igarashi, S.; Yamano, A.; Sato, S. *Chem. Commun.* **1997**, 711; (b) Doble, D. M. J.; Benison, C. H.; Blake, A. J.; Fenska, D.; Jackson, M. S.; Kay, R. D.; Li, W.-S.; Schroder, M. *Angew. Chem., Int. Ed.* **1999**, 38, 1915. (c) Zhang, J.-J.; Hu, S.-M.; Zheng, L.-M.; Wu, X.-T.; Fu, Z.-Y.; Dai, J.-C.; Du, W.-X.; Zhang, H.-H.; Sun, R.-Q. *Chem.–Eur. J.* **2002**, 8, 5742; (d) Liu, Q.-D.; Gao, S.; Li, J.-R.; Zhou, Q.-Z.; Yu, K.-B.; Ma, B.-Q.; Zhang, S.-W.; Zhang, X.-X.; Jin, T.-Z. *Inorg. Chem.* **2000**, 39, 2488; (e) Zhang, Y.-J.; Ma, B.-Q.; Gao, S.; Li, J.-R.; Liu, Q.-D. *J. Chem. Soc., Dalton Trans.* **2000**, 2249; (f) Tasiopoulos, A. J.; Wernsdorfer, W.; Moulton, B.; Zaworotko, M. J.; Christou, G. *J. Am. Chem. Soc.* **2003**, 125, 15274.
- (10) Wang, S. N.; Pang, Z.; Wagner, M. J. *Inorg. Chem.* **1992**, 31, 5381.
- (11) Chen, X.-M.; Aubin, S. M. J.; Wu, Y.-L.; Yang, Y.-S.; Mak, T. C. W.; Hendrickson, D. N. *J. Am. Chem. Soc.* **1995**, 117, 9600.

cluster,¹² and one 32-nuclear La₆Cu₂₆ cluster¹³ have been reported. Carboxylic acid has been widely used as the ligand to construct 3d–4f clusters, but the largest cluster obtained with it as the ligand is only 18-nuclear¹¹. Therefore, the design and synthesis of high-nuclear 3d–4f clusters are still significant.

Amino acids are some of the most important biological ligands, and metal ions are known to participate in a variety of biological reactions; therefore, research on the coordination behavior of metal–amino acid complexes is one of the most essential elements of chemical biology. Until now many Ln–amino acid complexes¹⁴ and 1:1 or 1:2 transition-metal–amino acid complexes¹⁵ with mononuclear or chain structure motif have been synthesized, though only recently, a series of polynuclear lanthanide clusters with amino acid as the ligand were reported (most of them display a Ln₄O₄-cubane structural motif).¹⁶ It is also shown that amino acids are useful ligands for the construction of polynuclear copper clusters.¹⁷

Recently, our research interest has been focused on the syntheses of high-nuclear 3d–4f heterometallic clusters with an amino acid as a ligand.^{9(c),13} In this paper, we will show that if glycine (or L-alanine) and acetic acid were used as ligands then 30-nuclear clusters [Sm₆Cu₂₄(μ₃-OH)₃₀(Gly)₁₂(Ac)₁₂(ClO₄)(H₂O)₁₆]·(ClO₄)₉·(OH)₂·(H₂O)₃₁ (**1**) and [Ln₆Cu₂₄(μ₃-OH)₃₀(Ala)₁₂(Ac)₆(ClO₄)(H₂O)₁₂]·(ClO₄)₁₀·(OH)₇·(H₂O)₃₄ (**2**·Ln) (Ln = Tb, Gd, Dy, Sm, and La) can be obtained. All of these clusters have a Ln₆Cu₂₄ metal skeleton. The crystal structures of **1** and **2**·Tb have been discussed. The temperature dependence of magnetic susceptibilities of **2**·Ln was investigated and was found to vary with the central rare-earth ions. Impedance spectroscopic measurements of **2**·Ln reveal that that it is an ionic conductor.

Results and Discussion

Syntheses. The strategy for the syntheses of high-nuclear 3d–4f clusters in this paper is to utilize appropriate chelating ligands (in this paper amino acid) to control the hydrolysis of 3d and 4f metal ions. The difficulty of this strategy is seeking a suitable pH window so that the amino acid ligand can use both its amino and carboxylate groups to coordinate to 3d and 4f metal ions simultaneously. We found that 6.6 is a suitable pH value. Higher pH values will lead to a large amount of precipitate and are not preferred. Another key role is the reactant proportion. We found that it is necessary to maintain a high metal to ligand ratio because a low ratio

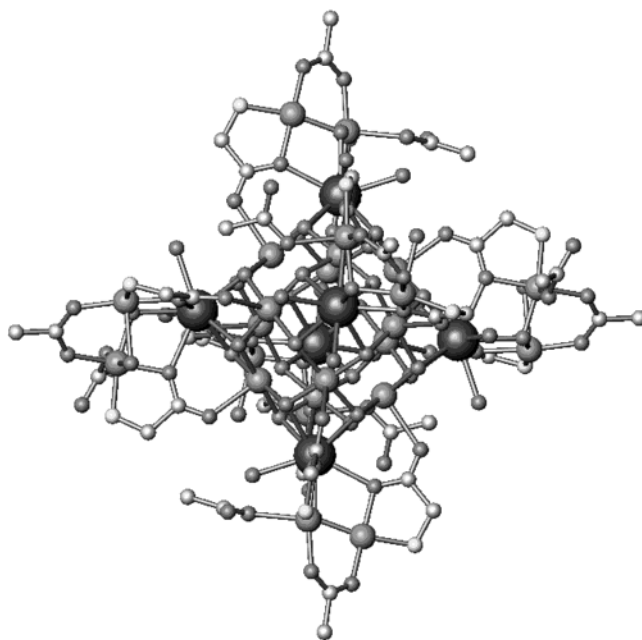


Figure 1. Structure of the cation of **1**. (The captured ClO₄[−] ion is omitted for clarity.)

Table 1. Crystallographic and Data Collection Parameters for **1** and **2**·Tb

	1	2 ·Tb
formula	C ₄₈ H ₂₁₀ Cl ₁₀ Cu ₂₄ ·N ₁₂ O ₁₆₇ Sm ₆	C ₄₈ H ₂₁₉ Cl ₁₁ Cu ₂₄ ·N ₁₂ O ₁₆₃ Tb ₆
M _r	6427.86	6513.85
cryst syst	Triclinic	Triclinic
space group	P $\bar{1}$	P $\bar{1}$
a/Å	16.251(3)	18.7910(2)
b/Å	18.415(4)	18.8588(3)
c/Å	19.481(4)	19.8593(1)
α/deg	114.62(3)	101.12
β/deg	110.55(3)	103.046(1)
γ/deg	95.69(3)	119.744(1)
vol/Å ³	4752.1(17)	5552.69(11)
Z	1	1
d _{calcd} , g/cm ³	2.240	1.926
F(000)	3156	3168
measured reflns	51063	28765
independent reflns	21000	19304
R(int)	0.0289	0.0291
GOF on F ²	1.057	1.153
R ^a	0.0456	0.0693
R _w ^b	0.1218	0.1830

^a $R = \sum(|F_o| - |F_c|) / \sum|F_o|$. ^b $R_w = \{\sum w[(F_o^2 - F_c^2)^2] / \sum w(F_o^2)^2\}^{1/2}$, $w = 1/[\sigma^2(F_o^2) + (aP)^2 + bP]$, $P = (F_o^2 + 2F_c^2)/3$. **1**, $a = 0.0567$, $b = 52.7538$; **2**·Tb, $a = 0.0868$, $b = 91.3996$.

(such as Ln/Cu/Gly/Ac = 1:4:2:2) will lead to the final product being contaminated by a small number of light-blue helix crystals (X-ray structure analysis shows it is Cu₃(Gly)₄(ClO₄)₂).

Description of Structures. The molecular structure of **1** in the solid state was determined by X-ray crystallography at 103 K, and the structure of the cation is shown in Figure 1. Selected bond distances and angles are shown in Tables 2 and 3, respectively. Figure 2 shows that the inner core of cation of **1** may be described as a huge octahedron with pseudocubic *O_h* symmetry. Six Sm^{III} ions with an average distance of about 7 Å are located at the vertices of a nonbonding octahedron, and the 12 inner Cu^{II} ions are located

- (12) Blake, A. J.; Gould, R. O.; Grant, C. M.; Milne, P. E. Y.; Parsons, S.; Winpenny, R. E. P. *J. Chem. Soc., Dalton Trans.* **1997**, 485.
- (13) (a) Hu, S.-M.; Dai, J.-C.; Wu, X.-T.; Wu, L.-M.; Cui, C.-P.; Fu, Z.-Y.; Hong, M.-C.; Liang, Y.-C. *J. Cluster Sci.* **2002**, *13*, 33. (Included in the special memorial issue in honor of Professor Jia-Xi Lu, the founder of Fujian Institute of Research on the Structure of Matter). (b) Zhang, J.-J.; Xia, S.-Q.; Sheng, T.-L.; Hu, S.-M.; Leibeling, G.; Meyer, F.; Wu, X.-T.; Xiang, S.-C.; Fu, R.-B. *Chem. Commun.* **2004**, 1186.
- (14) Wang, R. Y.; Gao, F.; Jin, T.-Z. *Huaxue Tongbao* **1996**, *10*, 14.
- (15) Ohata, N.; Masuda, H.; Yamauchi, O. *Angew. Chem., Int. Ed. Engl.* **1996**, *35*, 531, and references therein.
- (16) (a) Zheng, Z.-P. *Chem. Commun.* **2001**, 2521. (b) Ma, B.-Q.; Zhang, D.-S.; Gao, S.; Jin, T.-Z.; Yan, C.-H.; Xu, G.-X. *Angew. Chem., Int. Ed.* **2000**, *39*, 3644–3646.
- (17) Hu, S.-M.; Du, W.-X.; Dai, J.-C.; Wu, L.-M.; Cui, C.-P.; Fu, Z.-Y.; Wu, X.-T. *J. Chem. Soc., Dalton Trans.* **2001**, 2963–2964.

Table 2. Selected Bond Lengths (Å) for **1**

Sm ^{III} •••Sm	6.925–7.000	Cu(outer)•••Cu(outer)	2.990–3.045
Sm ^{III} •••Cu(inner)	3.442–3.520	Sm–O(water)	2.446(4)–2.470(4)
Sm ^{III} •••Cu(outer)	3.545–3.594	Sm–O(OH)	2.406(3)–2.484(4)
Cu(inner)•••Cu(inner)	3.252–3.419	Sm–O(carboxylate)	2.522(4)–2.557(4)
Cu(inner)–O(OH)	1.940(3)–1.982(4)	Cu(inner)–O(carboxylate)	2.319(4)–2.456(4)
Cu(7)–N(1)	1.986(5)	Cu(10)–N(4)	1.980(5)
Cu(7)–O(1)	1.971(4)	Cu(10)–O(7)	1.994(4)
Cu(7)–O(14)	1.949(4)	Cu(10)–O(15)	1.965(4)
Cu(7)–O(43)	1.943(4)	Cu(10)–O(44)	1.941(4)
Cu(7)–O(56)	2.312(4)	Cu(10)–O(57)	2.410(5)
Cu(8)–N(3)	1.992(4)	Cu(11)–N(6)	1.997(5)
Cu(8)–O(5)	1.994(4)	Cu(11)–O(11)	1.987(4)
Cu(8)–O(13)	1.985(4)	Cu(11)–O(17)	1.948(4)
Cu(8)–O(19)	2.245(4)	Cu(11)–O(45)	1.947(4)
Cu(8)–O(43)	1.950(3)	Cu(12)–N(5)	1.989(5)
Cu(9)–N(2)	1.997(4)	Cu(12)–O(9)	1.981(3)
Cu(9)–O(3)	1.983(4)	Cu(12)–O(18)	1.965(4)
Cu(9)–O(16)	1.956(4)	Cu(12)–O(23)	2.260(4)
Cu(9)–O(21)	2.349(5)	Cu(12)–O(45)	1.956(4)
Cu(9)–O(44)	1.966(4)		

Table 3. Selected Bond Angles (deg) for **1**

O(31)–Sm(1)–O(43)	120.31(12)	O(13)–Cu(8)–N(3)	96.69(17)
O(31)–Sm(1)–O(54)	139.40(12)	O(13)–Cu(8)–O(5)	168.06(16)
O(38)–Sm(1)–O(36)	102.75(13)	O(16)–Cu(9)–O(3)	168.48(18)
O(31)–Sm(1)–O(37)	100.00(12)	O(44)–Cu(9)–N(2)	168.10(17)
O(31)–Sm(1)–O(55)	141.20(13)	O(3)–Cu(9)–N(2)	84.27(17)
O(54)–Sm(1)–O(1)	136.71(13)	O(44)–Cu(10)–N(4)	167.1(2)
O(37)–Sm(1)–O(1)	137.69(12)	O(15)–Cu(10)–N(4)	96.6(2)
O(31)–Sm(1)–O(5)	73.99(12)	O(15)–Cu(10)–O(7)	174.59(17)
O(37)–Sm(1)–O(5)	133.51(12)	O(17)–Cu(11)–O(11)	175.08(17)
O(55)–Sm(1)–O(5)	135.19(12)	O(45)–Cu(11)–N(6)	168.98(17)
O(32)–Cu(1)–O(38)	177.70(15)	O(17)–Cu(11)–N(6)	96.01(19)
O(31)–Cu(1)–O(34)	176.99(15)	O(18)–Cu(12)–O(9)	169.79(16)
O(32)–Cu(1)–O(2)	91.01(14)	O(45)–Cu(12)–N(5)	169.88(17)
O(38)–Cu(1)–O(2)	87.62(15)	O(18)–Cu(12)–N(5)	95.36(18)
O(41) ^a –Cu(2)–O(32)	176.98(14)	Cu(7)–O(1)–Sm(1)	103.25(16)
O(33)–Cu(2)–O(40) ^a	177.71(15)	Cu(8)–O(5)–Sm(1)	103.66(14)
O(41) ^a –Cu(2)–O(4)	91.75(14)	Cu(3)–O(31)–Cu(1)	119.17(18)
O(32)–Cu(2)–O(4)	89.70(14)	Cu(3)–O(31)–Sm(1)	104.97(15)
O(31)–Cu(3)–O(42) ^a	177.81(15)	Cu(1)–O(31)–Sm(1)	103.01(15)
O(33)–Cu(3)–O(36)	178.73(14)	Cu(1)–O(32)–Cu(2)	116.29(17)
O(31)–Cu(3)–O(6)	89.97(15)	Cu(2)–O(33)–Cu(3)	110.76(17)
O(42) ^a –Cu(3)–O(6)	92.18(15)	Cu(6)–O(34)–Cu(1)	111.98(19)
O(36)–Cu(4)–O(40)	174.97(15)	Cu(6)–O(35)–Cu(5)	115.31(19)
O(39) ^a –Cu(4)–O(37)	176.49(15)	Cu(4)–O(36)–Cu(3)	118.39(18)
O(36)–Cu(4)–O(8) ^a	94.45(14)	Cu(4)–O(36)–Sm(1)	105.68(15)
O(40)–Cu(4)–O(8) ^a	90.57(14)	Cu(3)–O(36)–Sm(1)	102.67(15)
O(38)–Cu(5)–O(41)	177.16(16)	Cu(4)–O(37)–Cu(5)	119.17(18)
O(35)–Cu(5)–O(37)	177.69(15)	Cu(4)–O(37)–Sm(1)	104.48(15)
O(38)–Cu(5)–O(10) ^a	92.32(16)	Cu(5)–O(37)–Sm(1)	103.54(15)
O(35)–Cu(5)–O(10) ^a	90.00(15)	Cu(5)–O(38)–Cu(1)	113.82(19)
O(35)–Cu(6)–O(39)	179.17(15)	Cu(5)–O(38)–Sm(1)	105.27(16)
O(34)–Cu(6)–O(42)	178.59(15)	Cu(1)–O(38)–Sm(1)	101.94(15)
O(43)–Cu(7)–O(14)	96.52(16)	Cu(7)–O(43)–Cu(8)	100.40(16)
O(14)–Cu(7)–O(1)	178.17(17)	Cu(7)–O(43)–Sm(1)	107.39(16)
O(43)–Cu(7)–N(1)	163.6(2)	Cu(8)–O(43)–Sm(1)	108.44(15)
O(14)–Cu(7)–N(1)	94.8(2)	Cu(10)–O(44)–Cu(9)	101.74(17)
O(1)–Cu(7)–N(1)	83.74(19)	Cu(11)–O(45)–Cu(12)	102.68(17)
O(43)–Cu(8)–N(3)	166.44(16)		

^a Symmetry transformations used to generate equivalent atoms: $-x + 1, -y + 1, -z + 1$.

at the midpoints of the octahedral edges. The average Sm^{III}•••Cu and Cu•••Cu distances are 3.5 and 3.4 Å, respectively. Twenty-four μ_3 -OH⁻ groups, each one linking one Sm^{III} and two Cu^{II} ions, were used to construct the framework. Each surface of the octahedron is composed of three lanthanide ions and three Cu^{II} ions linked by three μ_3 -OH⁻ groups; therefore, the octahedron could also be imagined as being composed of Sm–O–Cu–O quadrilateral

(about 2.4×2 Å²) and Cu₃–O₃ (about 2 Å) distorted hexagonal windows.

Each cation also has 12 outer Cu^{II} ions. Each Sm^{III} ion interconnects two outer Cu^{II} ions with the help of one outer μ_3 -OH⁻ and two [3.1₁2₂₃1₃]-coordinated glycinato ligands. The average Sm^{III}•••Cu(outer) distance is about 3.5 Å, whereas that of Cu(outer)•••Cu(outer) is 3.0 Å, shorter than that of Cu(inner)•••Cu(inner). Short distances may cause strong magnetic exchanges between copper ions.

The coordination polyhedron of the nine-coordinated Sm^{III} ion with an O₉ donor set may be best described as a monocapped square antiprism (Figure 3). The Sm^{III} ion coordinates to four inner μ_3 -OH⁻ groups (lower plane), two carboxylate oxygen atoms, two water molecules (upper plane), and one outer μ_3 -OH⁻ “cap”. The Ln–O bond distances are in the range of 2.44–2.57 Å. The inner Cu^{II} ion has a slightly distorted six-coordinated octahedral configuration with an O₆ donor set. (The equatorial plane is determined by four μ_3 -OH⁻ with Cu–O bond distances of about 2 Å, whereas the apical places are occupied by two oxygen atoms from one ClO₄⁻ and one carboxylate group, respectively, with Cu–O bond distances of about 2.3–2.4 Å.) Figure 4 shows the structure of one of the vertices of the octahedron of **1**. Of the 12 outer Cu^{II} ions, 2 (Cu11, Cu11A) have four-coordinated square-planar geometry and an NO₃ donor set that consists of 1 amino nitrogen atom and 1 carboxylate oxygen atom from glycine, 1 carboxylate oxygen atom from the acetate ligand, and 1 outer μ_3 -OH⁻. The bond distances are in the range of 1.94–2.0 Å. Cu7 and Cu7A adopt five-coordinated NO₄ square-pyramidal geometry, whose square plane is determined by the NO₃ donor set, just as that of Cu11 and the apical plane is occupied by a water molecule. The other copper ions (Cu8, Cu8A, Cu9, Cu9A, Cu12, and Cu12A) also have five-coordinated NO₄ square-pyramidal geometries as does of Cu7 except that the apical plane is occupied by a carboxylate oxygen atom from the acetate ligand.

The glycinato ligand adopts a [3.1₁2₂₃1₃]-coordinated mode, chelating to two Cu^{II} ions and one Sm^{III} ion through the carboxylate and amino groups (Scheme 1). For the acetate ligand, two coordination modes are observed; that is, six are

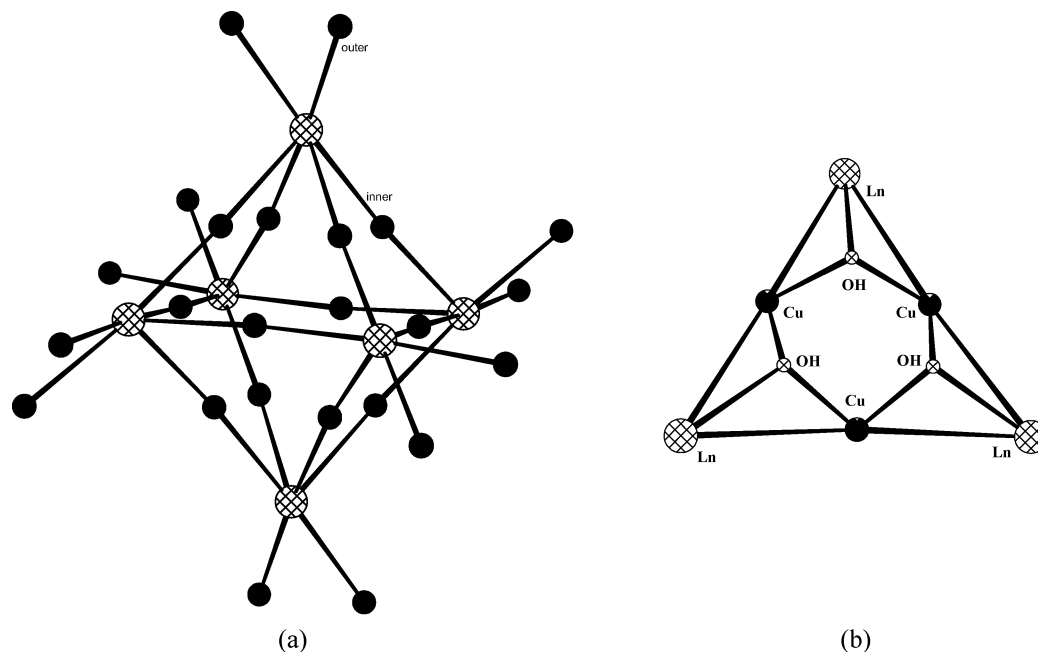


Figure 2. (a) Metal framework of the cations of **1** and **2·Tb**; ● denotes Cu and a hatched circle denotes Ln. (b) Structure of one face of the octahedron.

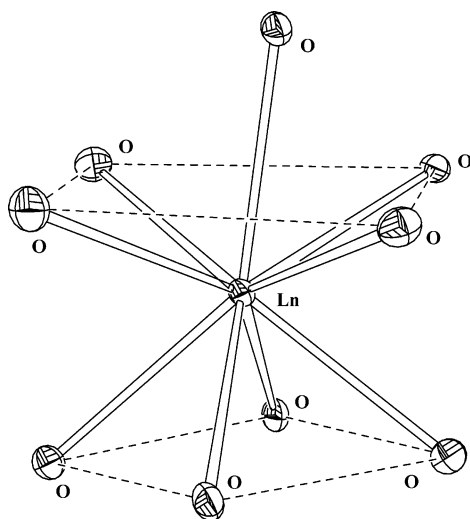


Figure 3. Coordination polyhedron of the Ln^{3+} ion in **1** and **2·Tb**.

bidentate and each coordinates to two neighboring outer Cu^{II} ions, whereas the other six are monodentate and each coordinates to one outer Cu^{II} ion.

A particularly interesting structural feature of this $\{\text{Sm}_6\text{Cu}_{24}\}$ cluster is the encapsulated distorted ClO_4^- anion at the center of the octahedral cage (The anion uses oxygen atoms coordinated to the inner copper ions). Confirmation of the template role of this ClO_4^- in the self-assembly process is demonstrated by the inability to form analogous cage structures with chloride as the anion. Previous authors have shown that a template ClO_4^- is essential for the syntheses of $\text{Ln}_6\text{Cu}_{12}$ clusters.^{11,19} Now, we provide another elegant demonstration of the under-appreciated potential role of the

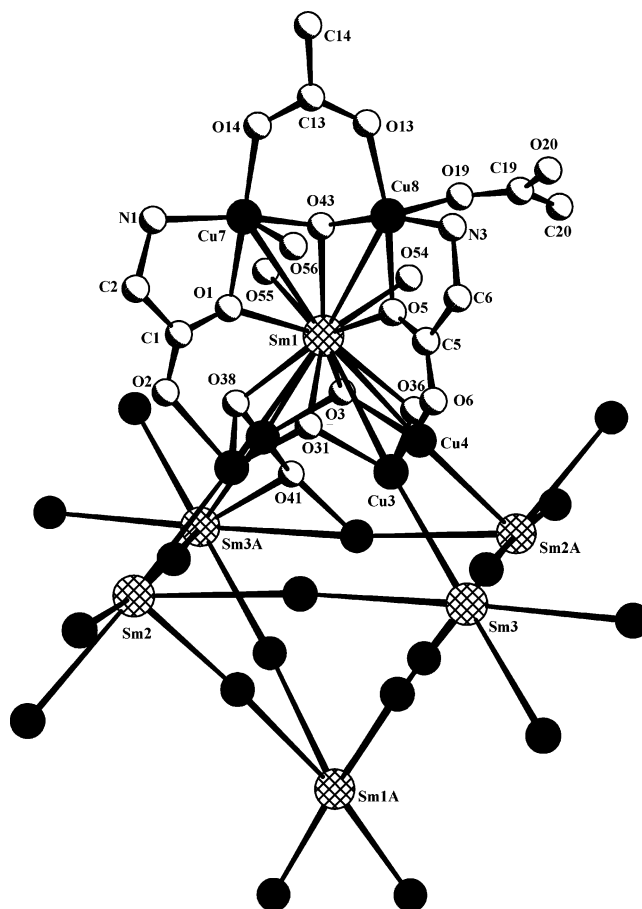


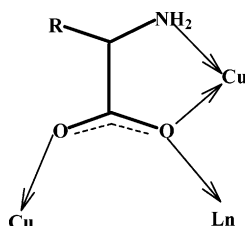
Figure 4. Stereoview of the structure of one of the vertices of the octahedron of **1**.

anions in the self-assembly process. Another structural feature of the cluster is the large size (with dimensions of about $2.38 \times 2.38 \times 2.38 \text{ nm}^3$). This size is significantly larger than that of the famous Mn_{12} cluster⁵ and comparable with that of the Mn_{30} cluster.⁶

- (18) Coxall, R. A.; Harris, S. G.; Henderson, D. K.; Parsons, S.; Tasker, P. A.; Winpenny, R. E. *J. Chem. Soc., Dalton Trans.* **2000**, 2349.
 (19) (a) Yang, Y.-Y.; Chen, X.-M.; Ng, S.-W. *J. Solid State Chem.* **2001**, *161* (2), 214–224. (b) Chen, X.-M.; Wu, Y.-L.; Tong, Y.-X.; Huang, X.-Y. *J. Chem. Soc., Dalton Trans.* **1996**, 2443. (c) Cui, Y.; Chen, J.-T.; Huang, J.-S. *Inorg. Chim. Acta* **1999**, *293*, 129.

Table 4. Selected Bond Lengths (Å) for **2**·Tb

Tb···Tb	6.929–9.953	Cu(outer)···Cu(outer)	2.988–3.006
Tb···Cu(inner)	3.439–3.503	Cu(inner)···Cu(inner)	3.295–3.405
Tb···Cu(outer)	3.531–3.553	Tb–O(OH)	2.388(7)–2.455(7)
Tb–O(water)	2.414(8)–2.442(8)	Tb–O(carboxylate)	2.516(8)–2.528(8)
Cu(inner)–O(OH)	1.946(7)–1.981(7)	Cu(inner)–O(carboxylate)	2.296(9)–2.384(8)
Cu(7)–O(19)	1.929(11)	Cu(10)–O(43)	1.938(8)
Cu(7)–O(9)	1.954(8)	Cu(10)–O(21)	1.967(8)
Cu(7)–O(42)	1.960(9)	Cu(10)–O(1)	1.981(8)
Cu(7)–N(5)	1.973(12)	Cu(10)–N(1)	1.980(11)
Cu(8)–O(42)	1.951(8)	Cu(11)–O(23)	1.924(9)
Cu(8)–O(20)	1.953(9)	Cu(11)–O(44)	1.949(8)
Cu(8)–O(7)	1.969(7)	Cu(11)–O(5)	1.965(8)
Cu(8)–N(4)	1.998(13)	Cu(11)–N(3)	1.965(11)
Cu(9)–O(22)	1.923(9)	Cu(12)–O(24)	1.940(10)
Cu(9)–O(3)	1.958(8)	Cu(12)–O(44)	1.947(8)
Cu(9)–O(43)	1.965(8)	Cu(12)–O(11)	1.962(7)
Cu(9)–N(2)	1.970(10)	Cu(12)–N(6)	1.988(13)

Scheme 1. [3.1₁2₂₃1₃]-Coordination Mode of the Amino Acid Ligand Indicated by Harris Notation¹⁸

X-ray structure analyses showed that **2**·Ln compounds are isomorphous, so only the structure of **2**·Tb is reported here as an example. The structure of **2**·Tb is almost the same as that of **1** except that L-alanine was used to replace the glycinate ligand and only six bidentate acetate ligands are used to construct the structure (each coordinates to two outer Cu^{II} ions just as that of **1**). Selected bond distances and angles are shown in Tables 4 and 5, respectively. Figure 5 shows the structure of one of the vertices of the octahedron of **2**·Tb. The coordination environments of Ln^{III} and inner Cu²⁺ are also almost the same as that of **1**, but that of the outer Cu^{II} ions are different. The 12 outer Cu^{II} ions of **2**·Tb all have four-coordinated square-planar geometry just as Cu7 of **1**. It should be noted that the methyl group of the L-alaninato ligand was found to be disordered.

The use of an amino acid instead of the widely used simple carboxylic acids for the synthesis of 3d–4f heterometallic clusters can bring an amino group into the system, which makes the structures obtained much more complex and intriguing than those composed of carboxylic acids. In fact, the structure of the Ln₆Cu₁₂ inner core is similar to the {Ln₆Cu₁₂} cluster with an η₂-coordinated betaine as the ligand.¹¹ But because amino acids have more coordination modes than the betaine ligand, this lead to the structures of the complexes reported here having much more beauty and being more intriguing than the OD 18-nuclear complex: the [3.1₁2₂₃1₃]-coordinated mode of the amino acid ligands brings 12 more Cu²⁺ ions into the system, thus a higher-nuclear cluster is obtained.

Electrical Conductivity and Magnetic Properties. The impedance plots (–Z'' vs Z') of **2**·La, **2**·Sm, **2**·Gd, and **2**·Tb were recorded at room temperature (22 °C) and are shown in Figure 6. Using **2**·Tb as an example, the measurement resulted in a typical behavior of an ionic conductor

Table 5. Selected Bond Angles (deg) for **2**·Tb

O(39)–Tb(1)–O(51)	138.4(3)	O(42)–Cu(8)–N(4)	167.7(4)
O(36)–Tb(1)–O(33)	100.0(2)	O(20)–Cu(8)–N(4)	97.9(5)
O(36)–Tb(1)–O(42)	130.1(3)	O(22)–Cu(9)–O(3)	175.8(4)
O(39)–Tb(1)–O(52)	138.4(3)	O(3)–Cu(9)–N(2)	84.0(4)
O(42)–Tb(1)–O(52)	73.3(3)	O(43)–Cu(9)–N(2)	168.7(4)
O(42)–Tb(1)–O(32)	136.0(3)	O(43)–Cu(10)–N(1)	167.7(4)
O(33)–Tb(1)–O(9)	138.4(2)	O(21)–Cu(10)–N(1)	97.1(4)
O(36)–Tb(1)–O(7)	140.7(3)	O(21)–Cu(10)–O(1)	172.0(4)
O(32)–Tb(1)–O(7)	134.6(3)	O(23)–Cu(11)–O(5)	174.0(4)
O(31)–Cu(1)–O(33)	176.9(3)	O(44)–Cu(11)–N(3)	168.4(4)
O(34)–Cu(1)–O(32)	178.1(3)	O(5)–Cu(11)–N(3)	84.2(4)
O(31)–Cu(1)–O(2)	89.7(3)	O(24)–Cu(12)–O(11)	172.8(5)
O(33)–Cu(1)–O(2)	93.3(3)	O(44)–Cu(12)–N(6)	168.4(4)
O(30)–Cu(2)–O(40) ^a	179.0(3)	O(11)–Cu(12)–N(6)	84.8(4)
O(31)–Cu(2)–O(35)	178.5(3)	Cu(8)–O(7)–Tb(1)	103.8(3)
O(30)–Cu(2)–O(4)	91.8(3)	Cu(7)–O(9)–Tb(1)	104.0(3)
O(40) ^a –Cu(2)–O(4)	88.7(3)	Cu(2)–O(30)–Cu(3)	116.4(3)
O(36)–Cu(3)–O(30)	178.4(3)	Cu(3)–O(32)–Cu(1)	112.9(4)
O(37)–Cu(3)–O(32)	178.2(3)	Cu(3)–O(32)–Tb(1)	104.0(3)
O(37)–Cu(3)–O(6)	87.1(3)	Cu(1)–O(32)–Tb(1)	104.3(3)
O(36)–Cu(3)–O(6)	93.0(3)	Cu(1)–O(33)–Cu(4)	120.0(4)
O(39)–Cu(4)–O(41)	177.1(3)	Cu(1)–O(33)–Tb(1)	105.7(3)
O(35) ^a –Cu(4)–O(33)	178.0(3)	Cu(4)–O(33)–Tb(1)	102.9(3)
O(39)–Cu(4)–O(8)	89.0(3)	Cu(3)–O(36)–Cu(5)	116.8(4)
O(41)–Cu(4)–O(8)	93.9(3)	Cu(3)–O(36)–Tb(1)	105.8(3)
O(38)–Cu(5)–O(39)	178.3(3)	Cu(5)–O(36)–Tb(1)	103.2(3)
O(40)–Cu(5)–O(36)	178.3(3)	Cu(3)–O(37)–Cu(6)	117.5(4)
O(39)–Cu(5)–O(10)	87.9(3)	Cu(5)–O(38)–Cu(6)	114.2(3)
O(36)–Cu(5)–O(10)	88.4(3)	Cu(4)–O(39)–Cu(5)	116.5(4)
O(34) ^a –Cu(6)–O(37)	176.6(3)	Cu(1)–O(39)–Tb(1)	104.6(3)
O(41) ^a –Cu(6)–O(38)	177.8(3)	Cu(5)–O(39)–Tb(1)	103.3(3)
O(34) ^a –Cu(6)–O(12)	93.5(3)	Cu(8)–O(42)–Cu(7)	100.4(4)
O(37)–Cu(6)–O(12)	89.9(3)	Cu(8)–O(42)–Tb(1)	107.7(3)
O(19)–Cu(7)–O(9)	175.6(5)	Cu(7)–O(42)–Tb(1)	107.0(3)
O(9)–Cu(7)–N(5)	84.6(4)	Cu(10)–O(43)–Cu(9)	100.4(3)
O(42)–Cu(7)–N(5)	169.1(4)	Cu(12)–O(44)–Cu(11)	100.1(4)
O(20)–Cu(8)–O(7)	172.7(5)		

^a Symmetry transformations used to generate equivalent atoms: $-x + 1, -y + 1, -z + 1$.

with a semicircle at high frequencies (from 150 Hz to 300 KHz) and a linear spike at low frequencies (from 20 to 150 Hz). The sample resistance from this plot is 103 K Ω, giving a conductivity of 7.72×10^{-6} S cm⁻¹. **2**·La, **2**·Sm, and **2**·Gd show similar behavior. The sample resistances and conductivities for these complexes are 8.6, 20.2, and 45.8 K Ω and 9.25×10^{-5} , 3.94×10^{-5} , and 1.74×10^{-5} S cm⁻¹, respectively. Detailed work on the mechanism of the conductivities on this series of complexes is still in progress.

Temperature-dependent magnetic susceptibilities of complexes **2**·Tb, **2**·La, **2**·Sm, and **2**·Gd were measured in the ranges of 5–300 K (for **2**·Tb), 2–295 K (for **2**·La), 2–300

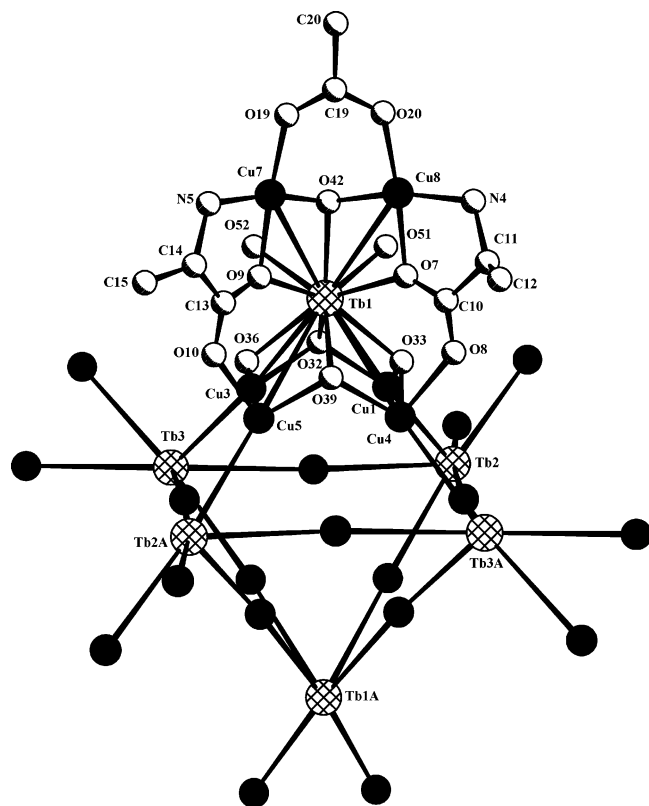


Figure 5. Stereoview of the structure of one of the vertices of the octahedron of 2·Tb.

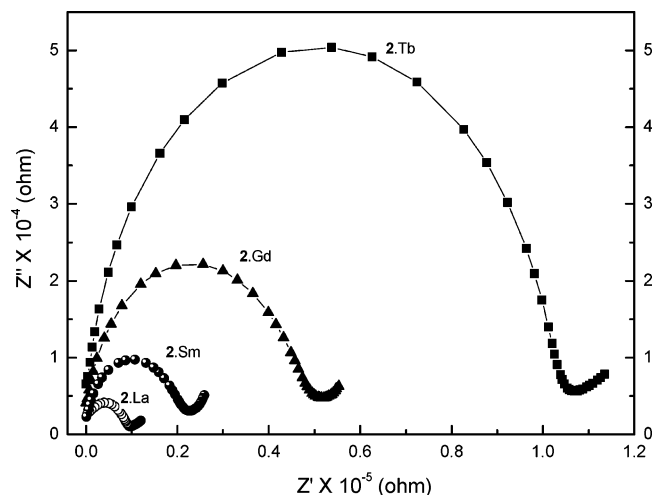


Figure 6. Impedance spectroscopy measurements of the electrical resistance of 2·Ln at room temperature.

K (for 2·Sm), and 5–300 K (for 2·Gd) and are shown in Figure 7. At room temperature, the $\chi_M T$ values per Ln₆Cu₂₄ unit are 9.3, 72.8, and 56.2 cm³ mol⁻¹ K for 2·La (295 K), 2·Tb (300 K), and 2·Gd (300 K), respectively, compared with the expected values (9.00, 79.88, and 56.25 cm³ mol⁻¹ K for 2·La, 2·Tb, and 2·Gd respectively) for 6 Ln^{III} in the free-ion state and 24 spin-only Cu^{II} ions ($S = 1/2$, $g = 2$). Upon cooling, 2·La shows a continuous decrease in $\chi_M T$, suggesting an overall antiferromagnetic coupling, as confirmed by the negative Weiss constant (−10.3 K). According to the literature¹¹, the Cu(inner)···Cu(inner) exchange interaction is antiferromagnetic. For the two neighboring outer Cu ions connected by a μ_3 -OH⁻ group and a carboxylate

group, because the \angle Cu(outer)–OH–Cu(outer) and the Cu(outer)···Cu(outer) distance are all about 100° and 3 Å, respectively, an antiferromagnetic interaction is also suggested.²⁰ 2·Sm also shows an overall antiferromagnetic interaction. The free-ion approximation for Sm(III) is not valid because of the presence of thermally populated excited states. The $\chi_M T$ value at room temperature is about 11.2 cm³ mol⁻¹ K. Considering that in the isostructural 2·La compound the 24 Cu(II) ions have been shown to contribute 9.3 cm³ mol⁻¹ K to the bulk value, it can be deduced from the total $\chi_M T$ value, and 0.32 cm³ mol⁻¹ K per Sm³⁺ ion is obtained. This value is close to the expected value for an isolated noninteracting Sm(III) ion.²¹

The magnetic behavior of 2·Gd is different from that of 2·La and 2·Sm. With the decrease in temperature, $\chi_M T$ remains almost constant down to ca. 75 K, where it begins to increase smoothly until reaching a maximum of 68 cm³ mol⁻¹ K around 5 K. This phenomenon corresponds to an overall ferromagnetic interaction, and the Weiss constant determined in the range of 50–300 K is 1.9 K. This also indicates that the magnetic interaction of Gd–Cu is ferromagnetic. The spin ground state of it is estimated to be $S = 11$ on the basis of the $\chi_M T$ value at 5 K.²² 2·Tb also shows an overall ferromagnetic interaction ($\theta = 0.59$ K).

Conclusions

In summary, with glycine and L-alanine as ligands, a series of 30-nuclear 3d–4f Ln₆Cu₂₄ compounds can be obtained through controlling the reactant to a reasonable proportion at a pH value of about 6.6. The use of amino acids instead of the widely used simple carboxylic acids for the synthesis of 3d–4f heteronuclear compounds brings an amino group into the system and makes the structures much more complex and intriguing than those composed of carboxylic acids. A “small” side chain (methyl group) of amino acid has led to some structural difference between 1 and 2. Therefore, a question arises: what clusters can we obtain if we use amino acids with large side chains or side chains containing O- or N-donor atoms as ligands? Future work on this subject is in progress.

Experimental Section

Materials and Instrumentation. Ln(ClO₄)₃·6H₂O complexes were synthesized by dissolving lanthanide oxide in an excess amount of perchloric acid. Other starting materials were of reagent grade and were used without further purification. Elemental analyses were carried out by the Elemental Analysis Lab of our Institute. Fluorescent spectra were measured with an Edinburgh FL-FS90 TCSPC system at the Spectroscopy Lab of Fuzhou University. Magnetic measurements were carried out with a Quantum Design PPMS model 6000 magnetometer.

Conductivity Measurements. The cylindrical pellets of the samples (0.1 cm in thickness and 0.4 cm in diameter) were coated with silver paint on either side. The conductivity measurements

(20) Crawford, V. H.; Richardson, H. W.; Wasson, J. R.; Hodgson, D. J.; Hatfield, W. E. *Inorg. Chem.* **1976**, *15*, 2107.

(21) Figgis, B. N.; Hitchman, M. A. *Ligand Field Theory and Its Applications*; Wiley-VCH: Toronto, 2000; Chapters 9 and 11.

(22) Brechin, E. K.; Harris, S. G.; Harrison, A.; Parsons, S.; Whittaker, A. G.; Winpenney, R. E. P. *Chem. Commun.* **1997**, 653.

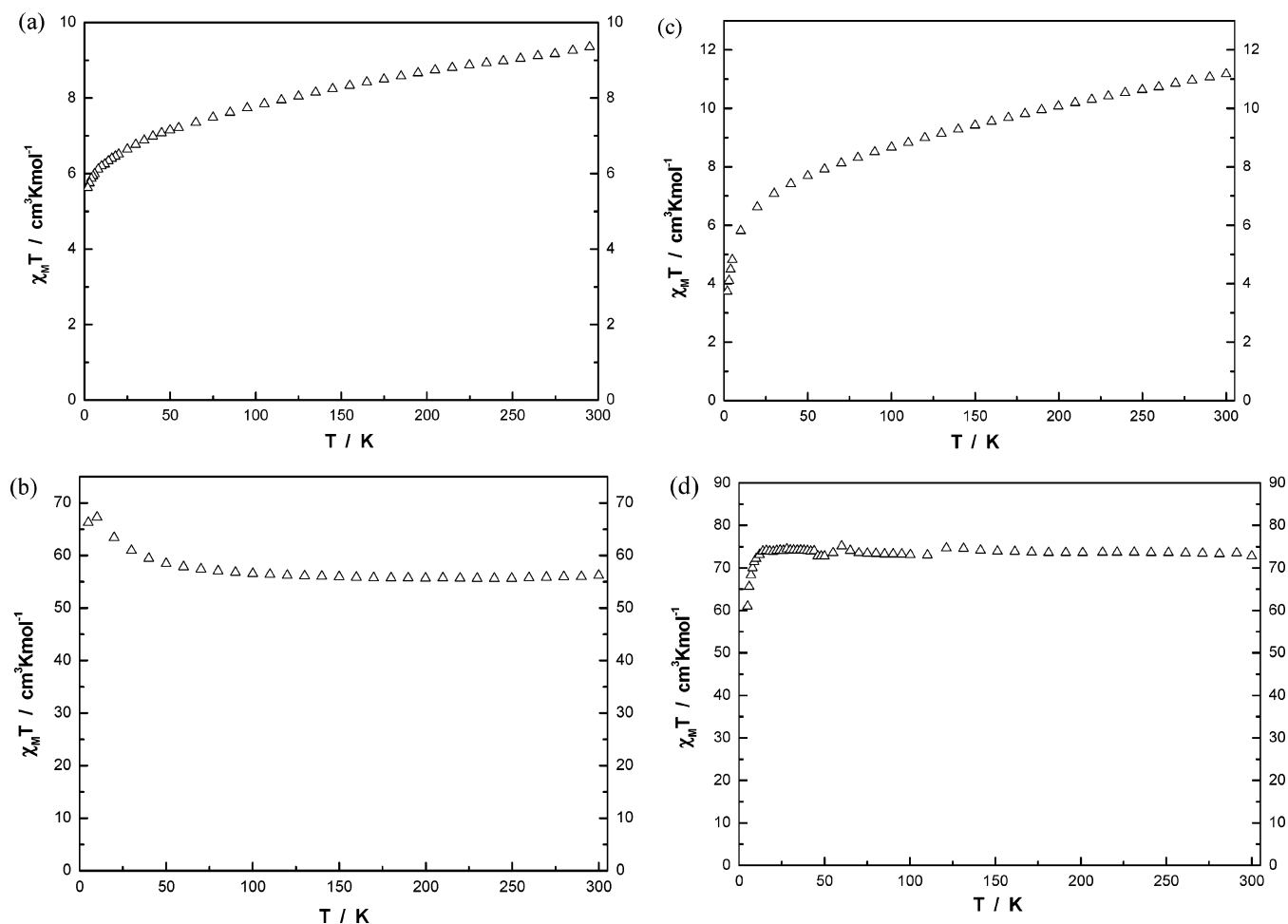


Figure 7. Temperature dependence of magnetic susceptibilities of $2\cdot\text{Ln}$. (a) $2\cdot\text{La}$, 2–295 K at 5000 G; (b) $2\cdot\text{Gd}$, 5–300 K at 5000 G; (c) $2\cdot\text{Sm}$, 2–300 K at 5000 G; (d) $2\cdot\text{Tb}$ (5–300 K at 10 000 G).

were carried out using a standard setup coupled with an Agilent 4284A LCR meter in the frequency range of 20 Hz to 1 MHz.

Synthesis of the Complexes. $[\text{Sm}_6\text{Cu}_{24}(\mu_3\text{-OH})_{30}(\text{Gly})_{12}(\text{Ac})_{12}(\text{ClO}_4)(\text{H}_2\text{O})_{16}] \cdot (\text{ClO}_4)_9 \cdot (\text{OH})_2 \cdot (\text{H}_2\text{O})_{31}$ (**1**) To an aqueous solution (10 mL) of $\text{Sm}(\text{ClO}_4)_3 \cdot 6\text{H}_2\text{O}$ (0.557 g, 1 mmol), we added $\text{Cu}(\text{ClO}_4)_2 \cdot 6\text{H}_2\text{O}$, $\text{NaAc} \cdot 3\text{H}_2\text{O}$, and glycine, and the proportion of the reactants was controlled to be $\text{Sm}^{3+}/\text{Cu}^{2+}/\text{Gly}/\text{Ac}^- = 1:6:1:4$. Then, the pH value of the reaction mixture was carefully adjusted to about 6.6 by the slow addition of a 0.1 M NaOH solution. After 2 h of stirring, we filtered the solution and placed it in a desiccator filled with phosphorus pentoxide. Blue crystals were obtained about a month later. The crystals were isolated by filtration, washed with cold water, and dried in the air. Yield, 0.22 g, 20.4%. Anal. Calcd for $\text{C}_{48}\text{H}_{210}\text{Cl}_{10}\text{Cu}_{24}\text{N}_{12}\text{O}_{167}\text{Sm}_6$: C, 8.99; H, 3.30; N, 2.62; Cl, 5.53. Found: C, 8.76; H, 3.14; N, 3.04; Cl, 5.72.

$[\text{Ln}_6\text{Cu}_{24}(\mu_3\text{-OH})_{30}(\text{Ala})_{12}(\text{Ac})_6(\text{ClO}_4)(\text{H}_2\text{O})_{12}] \cdot (\text{ClO}_4)_{10} \cdot (\text{OH})_7 \cdot (\text{H}_2\text{O})_{34}$ (**2**) ($\text{Ln} = \text{La}, \text{Sm}, \text{Gd}, \text{and Tb}$). The above procedure was repeated except that $\text{Ln}(\text{ClO}_4)_3 \cdot 6\text{H}_2\text{O}$, $\text{Cu}(\text{ClO}_4)_2 \cdot 6\text{H}_2\text{O}$, L-alanine, and $\text{NaAc} \cdot 3\text{H}_2\text{O}$ were used, and the proportion of the reactants was controlled to be $\text{Ln}^{3+}/\text{Cu}^{2+}/\text{Ala}/\text{Ac}^- = 1:6:1:4$. The yields are in the range of 20–32%. Anal. Calcd for $\text{C}_{48}\text{H}_{219}\text{Cl}_{11}\text{Cu}_{24}\text{N}_{12}\text{O}_{163}\text{Tb}_6$ (**2•Tb**): C, 8.95; H, 3.43; N, 2.61; Cl, 6.05. Found: C, 8.61; H, 3.27; N, 2.94; Cl, 6.42. Anal. Calcd for $\text{C}_{48}\text{H}_{219}\text{Cl}_{11}\text{Cu}_{24}\text{N}_{12}\text{O}_{163}\text{La}_6$ (**2•La**): C, 9.12; H, 3.49; N, 2.66. Found: C, 8.91; H, 3.37; N, 2.35. Anal. Calcd for $\text{C}_{48}\text{H}_{219}\text{Cl}_{11}\text{Cu}_{24}\text{N}_{12}\text{O}_{163}\text{Sm}_6$ (**2•Sm**): C, 9.02; H, 3.45; N, 2.63. Found: C, 8.77; H, 3.37; N, 2.46. Anal. Calcd for $\text{C}_{48}\text{H}_{227}\text{Cl}_{11}\text{Cu}_{24}\text{N}_{12}\text{O}_{167}\text{Gd}_6$ (**2•Gd**): C, 8.96; H, 3.43; N, 2.61. Found: C, 8.62; H, 3.40; N, 2.43.

X-ray Crystallography. Intensity data for **1** was collected on a Rigaku Mercury CCD area detector, and that for **2•Tb** was collected on a Siemens Smart/CCD area-detector diffractometer with Mo $K\alpha$ radiation ($\lambda = 0.71073 \text{ \AA}$). Data reduction and unit cell refinement were performed with Smart-CCD software.²³ The structures were solved by direct methods using SHELXS-97²⁴ and were refined by full-matrix least-squares methods using SHELXL-97. The anisotropic displacement parameters were refined for all non-hydrogen atoms except some of the oxygen atoms from free water molecules and ClO_4^- . Final $R = \sum(|F_o| - |F_c|)/\sum|F_o|$, $R_w = \{\sum w[(F_o^2 - F_c^2)^2]/\sum w[F_c^2]\}^{1/2}$, with $w = 1/[\sigma^2(F_o^2) + (aP)^2 + bP]$ (where $P = (F_o^2 + 2F_c^2)/3$). The crystallographic data are summarized in Table 1.

Acknowledgment. This research was supported by grants from the State Key Laboratory of Structural Chemistry, Fujian Institute of Research on the Structure of Matter, Chinese Academy of Sciences (CAS), the Ministry of Science and Technology of China (001CB1089), and the National Science Foundation (20333070, 20273073, 90206040) of China and Fujian Province (2002F014).

Supporting Information Available: Crystallographic data of **1** and **2•Tb** in CIF format. This material is available free of charge via the Internet at <http://pubs.acs.org>.

IC0497073

(23) XSCANS, version 2.1; Siemens Analytical X-ray Instruments Inc.: Madison, WI, 1994.

(24) Sheldrick, G. M.; *SHELXL-97, Program for X-ray Crystal Structure Refinement*; University of Göttingen: Göttingen, Germany, 1997.